

# Miscible Polymer Blend Dynamics: Double Reptation Predictions of Linear Viscoelasticity in Model Blends of Polyisoprene and Poly(vinyl ethylene)

Jai A. Pathak,<sup>†,§</sup> Sanat K. Kumar,<sup>‡,⊥</sup> and Ralph H. Colby<sup>\*,‡</sup>

Chemical Engineering Department and Materials Science and Engineering Department,  
The Pennsylvania State University, University Park, Pennsylvania 16802

Received February 24, 2004; Revised Manuscript Received June 25, 2004

**ABSTRACT:** Predictions of the linear viscoelastic complex shear modulus in model miscible blends of polyisoprene (PI) and poly(vinyl ethylene) (PVE) are compared with literature data. Using ideas of chain connectivity, the effective monomer relaxation times of PI and PVE in the blend were calculated using PI self-composition  $\phi_{PI,s} = 0.40$  and PVE self-composition  $\phi_{PVE,s} = 0.80$ , determined in our earlier analysis of segmental dynamics in PI/PVE blends. The reptation times of PI and PVE were then determined from their effective monomer relaxation times in the blend, assuming a common tube for both components (thus specifying the blend plateau modulus). The component reptation times and effective terminal dispersion widths from fits to the pure component polymers were input along with the blend plateau modulus to the des Cloizeaux “double reptation” model of polymer dynamics to make predictions of blend linear viscoelasticity with *no adjustable parameters*. The calculated frequency dependence of the complex modulus of PI/PVE blends was found to be in near quantitative agreement with experimental data, including the experimentally observed thermorheological complexity.

## 1. Introduction

Miscible polymer blend dynamics are complicated, as exemplified by the failure of the time–temperature superposition (tTS) principle.<sup>1–9</sup> While various theoretical models<sup>10–13</sup> have attempted to explain the underpinnings of these anomalies and to predict component segmental dynamics, to our knowledge there are no reported predictions of the linear viscoelastic complex modulus in miscible blends. The zero shear rate viscosity has been predicted but with rather limited success.<sup>14,15</sup> From the industrial perspective, this problem is important, as the ability to predict linear viscoelastic functions such as the zero shear viscosity will aid blend processing. To quantitatively predict the rheology of two-phase blends, it is imperative to first understand how the viscoelasticity of each phase depends on composition and temperature.

Our understanding of linear viscoelasticity (LVE) in entangled linear homopolymers is based on the tube model,<sup>16,17</sup> which has two parameters: the tube diameter and the monomer friction coefficient. The reptation model makes poor LVE predictions for polydisperse systems<sup>18,19</sup> because it ignores effects of surrounding chains on chain dynamics (constraint release). Early models of tube dilation, developed by Marrucci<sup>20</sup> and Viovy,<sup>21,22</sup> inspired the so-called “double reptation” theory, proposed independently by Tsenoglou<sup>23,24</sup> and des Cloizeaux.<sup>25–27</sup> Herein we use the des Cloizeaux version of double reptation, which has been shown to describe quantitatively LVE of melts containing two molecular weights of the same homopolymer.<sup>27</sup> The des

Cloizeaux double reptation model has also been successfully used to calculate LVE of entangled polydisperse polymer melts from the molecular weight distribution and the inverse problem.<sup>28–31</sup> While other models of constraint release do provide superior predictions,<sup>19,32</sup> double reptation has the advantage of being vastly easier to implement.

Mixing rules for the tube diameter only have subtle effects on predicted dynamics in miscible polymer blends<sup>5,6</sup> since the tube diameters of molten homopolymers that constitute common miscible blends are never more than a factor of 2 or so different from each other.<sup>33</sup> Indeed, a single tube may be assumed in miscible blends such as polyisoprene/poly(vinyl ethylene) (PI/PVE) blends.<sup>5</sup> Blending profoundly affects the friction coefficients of the components of a miscible blend.<sup>1,34–37</sup> This makes predictions of miscible blend dynamics more challenging than for polydisperse homopolymers. The monomer relaxation time  $\tau_{0,i}$  for component  $i$  in a miscible blend is intimately related to its monomer friction coefficient  $\zeta_{0,i}$ .<sup>38,39</sup>

$$\tau_{0,i} \cong \frac{\zeta_{0,i} b_i^2}{k_B T} \quad (1)$$

The Kuhn monomer length of component  $i$  is  $b_i$ , Boltzmann’s constant is  $k_B$ , and  $T$  is absolute temperature. All polymers have a distribution of segmental relaxation times that broadens considerably on blending.<sup>8</sup> While it is not obvious a priori how to select the effective monomer relaxation times needed for tube model predictions of terminal dynamics from the distributions of segmental times, we propose one possible approach here.

Zetsche and Fischer<sup>11</sup> proposed the first quantitative statistical mechanical theory for miscible blend segmental dynamics. Their model was modified by Kumar

<sup>†</sup> Chemical Engineering Department.

<sup>‡</sup> Materials Science and Engineering Department.

<sup>§</sup> Current address: Polymers Division, National Institute of Standards and Technology, Gaithersburg, MD 20899-8544.

<sup>⊥</sup> Current address: Department of Chemical and Biological Engineering, Rennselaer Polytechnic Institute, Troy, NY 12180.

\* Corresponding author. E-mail: rhc@plmsc.psu.edu.

et al.,<sup>12,40–42</sup> while drawing upon the ideas of Lodge and McLeish<sup>13</sup> on the influence of chain connectivity on segmental dynamics. Unfortunately, the segmental dynamics of miscible blends are not understood sufficiently to make quantitative predictions with no adjustable parameters. The Fischer/Kumar models correctly incorporate the role of concentration fluctuations but also rely on the concept of cooperative motion, which uses the increased cooperativity at lower temperatures to explain the divergence of relaxation times at the Vogel temperature ( $T_\infty$ ). However, at high temperatures (more than 50 K above the blend  $T_g$ ), which is typically where linear viscoelasticity measurements are made, Kant et al.<sup>42</sup> showed that ignoring concentration fluctuations only caused errors of less than 10% in the computed values of the mean segmental relaxation times in the mixture. Furthermore, the cooperative volume is small far above the blend  $T_g$ . Under these conditions, and only under these conditions, the concentration fluctuation models converge to the ideas of Lodge and McLeish,<sup>13</sup> in that the mean segmental relaxation times can be practically reproduced by simply incorporating the effects of chain connectivity alone.<sup>15,43,44</sup>

However, it has recently been shown that the additional assumption of Lodge and McLeish, that the cooperative length scale of relevance is sensibly equal to the Kuhn length of the chains, will not allow quantitative predictions of the temperature dependence of segmental dynamics in miscible blends,<sup>42</sup> particularly for the high- $T_g$  blend component. Kant et al.<sup>42</sup> have applied the Lodge–McLeish model in reverse to calculate the effective environment surrounding each blend component from measured segmental relaxation times. The low- $T_g$  blend component has a local environment that is consistent with  $T_\infty$  being determined on a local scale (of order the Kuhn length) at all temperatures and blend compositions. However, the high- $T_g$  component requires a temperature dependence of the local environment and hence the scale over which  $T_\infty$  is determined. This apparent asymmetry is not yet understood, but we use the Lodge–McLeish formalism with empirically determined self-compositions, owing to its simplicity, to calculate monomer relaxation times. While this description is adequate for our purposes here, where we only consider properties far above the blend glass transition temperature, this approach would have to be modified to incorporate the effects of concentration fluctuations if viscoelastic properties were considered at temperatures closer to  $T_g$ .

While we therefore consider the issue of segmental dynamics in miscible blends as an unsolved problem in polymer physics, here we show how to extend any description of segmental dynamics to make predictions of miscible blend LVE. The “description” could either be segmental relaxation time data or an empirical function describing segmental relaxation time data. We relate the effective monomer relaxation time to the peak of the distribution of segmental relaxation times. The effective monomer relaxation times, which control terminal relaxation of each component, were used to determine the reptation time.<sup>17</sup> These component reptation times were input to the des Cloizeaux double reptation model to determine the blend stress relaxation modulus  $G(t)$  and thence the complex modulus  $G^*(\omega)$ . Blend  $G^*(\omega)$  predictions have been tested against the experimental data of Zawada et al.<sup>5,45,46</sup> on PI/PVE blends comprising anionically polymerized components

(each having polydispersity index  $M_w/M_n < 1.1$ ), although the PI was a mixture of 94% polyisoprene and 6% perdeuterated polyisoprene of similar degrees of polymerization. This approach predicts miscible blend LVE with *no adjustable parameters*, as all parameters are extracted from fits to pure component literature data.

## 2. LVE Calculation Algorithm

### 2.1. Calculation of Component Reptation Times.

Since it is critical to determine the effective Kuhn monomer relaxation time for each blend component, we first calculated the effective local composition  $\phi_{\text{eff},i}$  for each component ( $i$  denotes PI or PVE), following the ideas of Lodge and McLeish.<sup>13</sup>

$$\phi_{\text{eff},i} = \phi_{s,i} + (1 - \phi_{s,i})\phi_i \quad (2)$$

For component  $i$ ,  $\phi_i$  is the macroscopic volume fraction and  $\phi_{s,i}$  is the self-composition from chain connectivity at the scale of the Kuhn length. The values of the self-composition  $\phi_s$  used here were 0.40 and 0.80 for PI and PVE, respectively, as determined by Kant et al.,<sup>42</sup> who found that while  $\phi_s$  is temperature invariant for the low- $T_g$  component, it increases with temperature for the high- $T_g$  component. This temperature dependence of  $\phi_{s,\text{PVE}}$  is a serious shortcoming of the mean-field model of Lodge and McLeish and effectively limits our LVE predictions to a narrow range of temperature. The  $\phi_{s,\text{PVE}}$  used here was determined by interpolating the  $\phi_s(T)$ , calculated by Kant et al., to  $T = 39^\circ\text{C}$  (where we make LVE predictions); see Figure 4a of ref 42. The  $\phi_{s,\text{PVE}} = 0.8$  determined by Kant et al. was significantly higher than the estimate of Lodge and McLeish, who determined  $\phi_{s,\text{PVE}} = 0.25$ . The value of  $\phi_{s,\text{PI}} = 0.40$  calculated by Kant et al. is in good agreement with the estimate of Lodge and McLeish, who calculated  $\phi_{s,\text{PI}} = 0.45$ .

These effective compositions were then used in the calculation of the effective Kuhn monomer relaxation time of each component  $\tau_{0,i}$ . We assumed that the WLF coefficients referenced to the glass transition in the blend are the pure component values ( $C_{1,i}^g$  and  $C_{2,i}^g$ ). For computing  $\tau_{0,\text{PI}}$ , the glass transition was taken to be that corresponding to the environment with  $\phi = \phi_{\text{eff},\text{PI}}$ , written as  $T_g(\phi_{\text{eff},\text{PI}})$ , which was determined using the Fox equation.<sup>47</sup>

$$\frac{1}{T_g(\phi_{\text{eff},\text{PI}})} = \frac{\phi_{\text{eff},\text{PI}}}{T_{g,\text{PI}}} + \frac{1 - \phi_{\text{eff},\text{PI}}}{T_{g,\text{PVE}}} \quad (3)$$

The final expression for  $\tau_{0,\text{PI}}$ , based on the WLF equation<sup>48</sup> is as follows:

$$\log\left(\frac{\tau_{0,\text{PI}}}{\tau_{g,\text{PI}}}\right) = \frac{-C_{1,\text{PI}}^g[T - T_g(\phi_{\text{eff},\text{PI}})]}{T - T_g(\phi_{\text{eff},\text{PI}}) + C_{2,\text{PI}}^g} \quad (4)$$

Here  $\tau_{g,\text{PI}}$  is the Kuhn monomer relaxation time of *pure* PI at  $T_g$ , determined from pure component rheology data in concert with experimental segmental dynamics data (discussed in detail with other pure component properties below). For calculating  $\tau_{0,\text{PVE}}$ ,  $T_g$  was determined

for an environment containing  $\phi_{\text{eff,PVE}}$  and  $\tau_{g,\text{PVE}}$  is the Kuhn monomer relaxation time of pure PVE at  $T_g$ .

$$\log\left(\frac{\tau_{0,\text{PVE}}}{\tau_{g,\text{PVE}}}\right) = \frac{-C_{1,\text{PVE}}^g [T - T_g(\phi_{\text{eff,PVE}})]}{T - T_g(\phi_{\text{eff,PVE}}) + C_{2,\text{PVE}}^g} \quad (5)$$

$T_g(\phi_{\text{eff,PVE}})$  was also determined using the Fox equation:

$$\frac{1}{T_g(\phi_{\text{eff,PVE}})} = \frac{\phi_{\text{eff,PVE}}}{T_{g,\text{PVE}}} + \frac{1 - \phi_{\text{eff,PVE}}}{T_{g,\text{PI}}} \quad (6)$$

The above descriptions of glass transition temperature and segmental relaxation time are widely used for miscible blend dynamics.<sup>15,42–44</sup>

The reptation times of PI  $\tau_{\text{rep,PI}}$  and PVE  $\tau_{\text{rep,PVE}}$  were then calculated from the effective monomer relaxation times.<sup>17,39</sup>

$$\tau_{\text{rep,PI}} = \frac{b_{\text{PI}}^2 N_{\text{PI}}^3}{[a(\phi)]^2} \tau_{0,\text{PI}} \quad (7)$$

$$\tau_{\text{rep,PVE}} = \frac{b_{\text{PVE}}^2 N_{\text{PVE}}^3}{[a(\phi)]^2} \tau_{0,\text{PVE}} \quad (8)$$

$N_i$  is the number of Kuhn monomers per chain of component  $i$ . The tube diameter in the blend  $a(\phi)$  was calculated using the single tube assumption,<sup>5,8</sup> using the pure component tube diameters  $a_{\text{PI}}$  and  $a_{\text{PVE}}$  of PI and PVE, respectively.

$$\frac{1}{a(\phi)} = \frac{\phi}{a_{\text{PI}}} + \frac{1 - \phi}{a_{\text{PVE}}} \quad (9)$$

$\phi$  is the macroscopic volume fraction of PI in the blend.

**2.2. Calculation of Stress Relaxation Modulus and Complex Modulus.**  $G(t)$  was calculated using the double reptation model of des Cloizeaux,<sup>27</sup> where the stress in a step strain experiment is determined by the fraction of original entanglements  $F(t)$  surviving at time  $t$ . In his model, the stress borne by an entanglement between any two chains is relaxed completely when either chain diffuses away. By solving a time-dependent diffusion equation for entanglement abandonment, des Cloizeaux derived  $F(t)$ .<sup>27</sup>

$$F(t) = \left( \frac{8}{\pi^2} \sum_{\text{odd } p} \frac{1}{p^2} \exp[-p^2 U(t)] \right)^2 \quad (10)$$

$$U(t) = \frac{t}{\tau_{\text{rep}}} + \frac{\beta M_e}{M} g\left[\frac{tM}{\tau_{\text{rep}}\beta M_e}\right] \quad (11)$$

$$g(x) = \sum_{m=0}^{\infty} \frac{1 - \exp(-m^2 x)}{m^2} \quad (12)$$

$\beta$  is a constant exceeding unity that specifies the width of the terminal dispersion. The  $\beta$  for each component was determined by fitting the double reptation model to pure component  $G''(\omega)$  data, and the value of  $\beta$  was then fixed for each component in the blend.

In double reptation, the blend stress relaxation modulus  $G(t)$  is quadratic in the volume fraction  $\phi$ .<sup>27</sup>

$$G(t) = G_N^0(\phi) [\phi F_{\text{PI}}(t) + (1 - \phi) F_{\text{PVE}}(t)]^2 \quad (13)$$

$G_N^0(\phi)$  is the composition-dependent blend plateau modulus, determined by eq 9.<sup>5,8,39</sup>

$$\frac{G_N^0(\phi)}{k_B T} = \left[ \frac{b_{\text{PI}}^2 \phi}{v_{0,\text{PI}}} + \frac{b_{\text{PVE}}^2 (1 - \phi)}{v_{0,\text{PVE}}} \right] \left[ \frac{\phi}{a_{\text{PI}}} + \frac{(1 - \phi)}{a_{\text{PVE}}} \right]^2 \quad (14)$$

The terms  $v_{0,\text{PI}}$  and  $v_{0,\text{PVE}}$  are the Kuhn monomer volumes of PI and PVE, respectively, defined as the ratio of the molar mass of a Kuhn monomer and the density.

Finally, the storage modulus  $G'(\omega)$  and loss modulus  $G''(\omega)$  of the blend were calculated from their definitions by spectral decomposition of  $G(t)$ .<sup>48</sup>

$$G'(\omega) = \omega \int_0^{\infty} G(t) \sin(\omega t) dt,$$

$$G''(\omega) = \omega \int_0^{\infty} G(t) \cos(\omega t) dt \quad (15)$$

Since analytical integration was precluded for  $G^*(\omega)$ , numerical Fourier transformation was performed by an efficient finite element approximation algorithm<sup>49</sup> (details in ref 50). For confidence, the FORTRAN code for calculating double reptation predictions of  $G^*(\omega)$  for blends and pure components was validated<sup>50</sup> against the published predictions of des Cloizeaux<sup>27</sup> on bidisperse 1,4-polybutadiene blends and pure component data.<sup>19</sup>

### 3. LVE Predictions and Discussion

**3.1. Double Reptation Fits to Pure Component Data.** Molecular characteristics (including weight-average molar mass  $M_w$ , polydispersity  $M_w/M_n$ , Kuhn length  $b$ , number of Kuhn monomers per chain  $N$ , glass transition temperature  $T_g$ , WLF coefficients  $C_1^g$  and  $C_2^g$ , and Kuhn monomer relaxation time  $\tau_g$  at  $T_g$  of PI and PVE used by Zawada et al.<sup>5,46</sup> are listed in Table 1. The Kuhn length  $b$  used here for calculating the molecular weight of a Kuhn monomer  $M_0$ , and hence  $N = M_w/M_0$ , was calculated in ref 50 using chain dimension data from ref 33. The  $T_g$ 's of the pure components were reported by Zawada.<sup>45</sup> The determination of  $\tau_g$  is described below. The  $v_{0,\text{PI}}$  and  $v_{0,\text{PVE}}$  (Kuhn monomer volumes of PI and PVE, respectively) were determined from the data provided by Balsara:<sup>51</sup> at 39 °C,  $v_{0,\text{PI}} = 202 \text{ \AA}^3$  and  $v_{0,\text{PVE}} = 545 \text{ \AA}^3$ .

The value of  $\beta$  is determined for PI and PVE by fitting the double reptation model of des Cloizeaux to the pure component data (see Figures 1 and 2, with fitting results in Table 2). The  $\beta$  values for PI and PVE in the blend are fixed to their pure component values in the implementation of double reptation for the blend. For PVE, the double reptation fit gave  $\beta = 9$ , while for 94% h-PI/6% d-PI the double reptation fit yielded  $\beta = 6$ . Double reptation is unable to quantitatively capture the correct width of the relaxation time distribution for the polymers, missing the data at the highest frequencies where contour length fluctuation effects<sup>39,52</sup> become important. For the h-PI–d-PI mixture, the double reptation fit yields  $G_N^0 = 3.35 \times 10^6 \text{ dyn cm}^{-2}$  ( $M_e = 6180$ ), in good agreement with the literature value ( $G_N^0 = 3.5 \times 10^6 \text{ dyn cm}^{-2}$ ).<sup>33</sup> For PVE, the double reptation fit to experimental data yields  $G_N^0 = 5.97 \times 10^6 \text{ dyn cm}^{-2}$  ( $M_e = 3680$ ), also in good agreement with the literature value ( $G_N^0 = 5.7 \times 10^6 \text{ dyn cm}^{-2}$ ).<sup>33</sup> The values of the tube diameter  $a (= \sqrt{M_e \langle R_0^2 \rangle / M})$  for PVE and h-PI/d-PI reported in Table 2 were calculated using unperturbed mean-squared end-to-end distance  $\langle R_0^2 \rangle / M$  data for PI



**Table 1. Weight-Average Molar Masses ( $M_w$ ), Polydispersities ( $M_w/M_n$ ), Kuhn Lengths ( $b$ ), Kuhn Monomer Molar Masses ( $M_0$ ), Number of Kuhn Segments per Chain ( $N = M_w/M_0$ ), WLF Parameters ( $C_1^g$  and  $C_2^g$ ),<sup>42</sup> Glass Transition Temperatures ( $T_g$ ),<sup>5</sup> and Monomer Relaxation Times at the Glass Transition Temperature ( $\tau_g$ , See Figure 3) of PI and PVE Samples Studied by Zawada et al.<sup>5</sup>**

polymer	$M_w$	$M_w/M_n$	$b$ (Å)	$M_0$	$N$	$T_g$ (°C)	$C_1^g$	$C_2^g$	$\tau_g$ (s)
PVE	204 000	<1.1	14	291	701	0.0	11.8	35.4	7.42
94% h-PI/6% d-PI	75 000 (h); 90 000 (d)	<1.1	8.2	110; 124	682; 726	-63.0	13.2	46.0	9.28

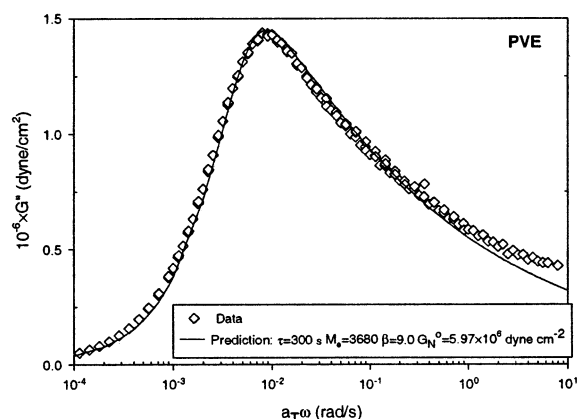


**Figure 1.** Double reptation fit to  $G''(\omega)$  data of Zawada et al.<sup>5</sup> for pure PVE at 39.4 °C.

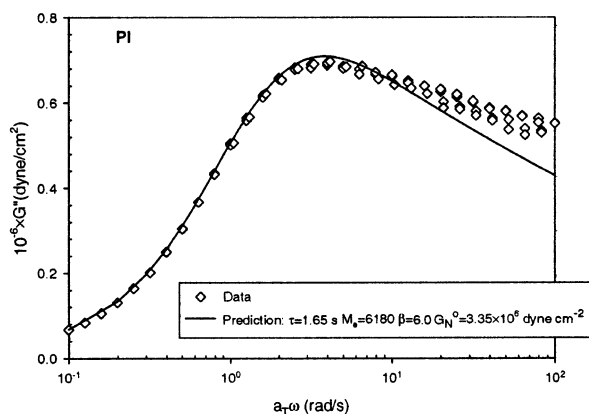


**Figure 2.** Double reptation fit to  $G''(\omega)$  data of Zawada et al.<sup>5</sup> for 94% hPI/6% d-PI at 2.3 °C.

**Table 2. Plateau Moduli ( $G_N^0$ ), Entanglement Strand Molar Masses ( $M_e$ ), Number of Kuhn Monomers in an Entanglement Strand ( $N_e$ ), des Cloizeaux  $\beta$  Factors, and Tube Diameters ( $a$ ) for PI and PVE from Fits in Figures 1 and 2**

polymer	$10^{-6} G_N^0$ (dyn cm <sup>-2</sup> )	$M_e$	$N_e$	$\beta$	$a$ (Å)
PVE	5.97	3680	12.7	9.0	49.6
94% h-PI/6% d-PI	3.35	6180	56.2	6.0	60.6

and PVE provided by Fetters et al.<sup>33</sup> All values of  $G_N^0$ ,  $M_e$ , and  $a$  used in this work are based on these double reptation fits to pure component data.

**3.2. Estimation of Monomer Relaxation Time at the Glass Transition Temperature.** We need  $\tau_g$  (the pure component Kuhn monomer relaxation time at  $T_g$ ) for PI and PVE to implement the WLF eqs 4 and 5. From the experimental terminal relaxation times of pure PI and pure PVE, we calculated the segmental time  $\tau_0$  by invoking reptation scaling with contour length fluctuations (the Doi model<sup>39,52</sup>) with terminal time ( $N_e^3/N_e,i$ )(1 -  $\sqrt{N_e,i/N_e}$ )<sup>2</sup> $\tau_{0,i}$ . Since oscillatory shear data showing the terminal relaxation are typically not available within 20 or 30 K of  $T_g$  (due to long relaxation

times), determining  $\tau_g$  poses a challenge. In addition, segmental and terminal relaxation times often have different temperature dependences (see ref 8 and refs 70–77 therein). Estimation of  $\tau_g$  requires an extrapolation of the calculated  $\tau_0$  from high temperatures to  $T_g$ . To boost our confidence in this extrapolation, we combined the calculated monomer times ( $\tau_0$ ) with experimentally measured segmental relaxation times (taken as the peak of the  $\alpha$ -relaxation in dielectric spectroscopy,  $\tau_\alpha$ ) on pure PI and PVE, since the latter are available at and near  $T_g$  and also across a broad temperature range. Since  $\tau_0$  is a slow segmental time that governs terminal relaxation, it exceeds  $\tau_\alpha$ .<sup>8</sup> By observation, we fixed the ratio  $\tau_0/\tau_\alpha$  and then used this constant to scale down  $\tau_0$  so that it fell on the same curve as  $\tau_\alpha$  when plotted vs  $T$ . For PI and PVE, the ratio  $\tau_\alpha/\tau_0$  equals 0.35 and 0.075, respectively. Thereafter, the WLF equation was fitted to these combined data to capture the temperature dependence of  $\tau_0$ . These WLF coefficients and the ratio  $\tau_0/\tau_\alpha$  were then used to extrapolate  $\tau_0$  to  $T_g$  to get  $\tau_g$ . The results of this procedure, which give  $\tau_{g,PI} = 9.28$  s and  $\tau_{g,PVE} = 7.42$  s, are shown in Figure 3. The different temperature dependences of segmental and terminal relaxation times make these determinations of effective monomer relaxation times only apply over a limited range of temperature (far above  $T_g$ , where terminal relaxation times are usually measured).

**3.3. Predictions of Blend LVE: Results.** Miscible blends of narrow molecular weight distribution polymers can exhibit two well-defined peaks in  $G''(\omega)$  which signify the terminal relaxation of the blend components.<sup>1–3,5,9,46,53</sup> The height and width of these peaks offer sharp features that enable sensitive tests of double reptation predictions against experimental data. We therefore compare the double reptation prediction of  $G''(\omega)$  with the corresponding experimental data, instead of making numerical comparisons between experimental and calculated values of zero shear viscosity  $\eta_0$ , which is simply the area under the  $G(t)$  curve:<sup>48</sup>  $\eta_0 = \int_0^\infty G(t) dt$ . If the component terminal relaxation times differ by less than a factor of 10, then these two peaks in  $G''(\omega)$  may not be resolved, e.g., in the data of Arendt et al.<sup>4</sup>

The peaks in  $G''(\omega)$  are quite clearly visible in the experimental data for the PVE/hPI–dPI mixture studied by Zawada et al.,<sup>5,46</sup> except in the blend containing  $\phi_{PVE} = 0.20$  (see Figures 4, 5, 6, and 7 for the experimental data and the double reptation predictions for blends with  $\phi_{PVE} = 0.20$ ,  $\phi_{PVE} = 0.40$ ,  $\phi_{PVE} = 0.60$ , and  $\phi_{PVE} = 0.80$ , respectively). In the  $\phi_{PVE} = 0.20$  blend, the relaxation peak at lower frequencies (due to PVE) is barely visible. The height of the lower frequency peak progressively increases with increasing  $\phi_{PVE}$ , and so we conclude that this peak is due to the terminal relaxation of PVE chains in the blend, implying that the high-frequency peak in  $G''(\omega)$  is due to the terminal relaxation of the PI chains in the blend. For all compositions, the terminal relaxation times of the two components (judged by the positions of the two  $G''(\omega)$  peaks on the

**Table 3. Composition ( $\phi_{\text{PVE}}$ ), Temperature ( $T$ ), and Calculated Values of Composition-Dependent Plateau Modulus  $G_N^0(\phi_{\text{PVE}})$ , Tube Diameter  $a$ , Effective Segmental Time  $\tau_{0,i}$  and Longest Relaxation Times  $\tau_{\text{rep},i}$  of Component  $i$  in the PVE/hPI–dPI Blends Studied by Zawada et al.<sup>5</sup>**

$\phi_{\text{PVE}}$	$T$ (°C)	$10^{-6} G_N^0$ (dyn cm <sup>-2</sup> )	$a$ (Å)	$\tau_{0,\text{PI}}$ (s)	$\tau_{\text{rep},\text{PI}}$ (s)	$\tau_{0,\text{PVE}}$ (s)	$\tau_{\text{rep},\text{PVE}}$ (s)
0.2	39.1	4.32	58.0	$1.34 \times 10^{-8}$	0.082	$8.17 \times 10^{-7}$	11.1
0.4	39.4	4.77	55.6	$2.06 \times 10^{-8}$	0.143	$1.15 \times 10^{-6}$	17.4
0.6	39.4	5.25	53.4	$3.51 \times 10^{-8}$	0.269	$1.73 \times 10^{-6}$	29.2
0.8	39.4	5.76	51.4	$6.54 \times 10^{-8}$	0.554	$2.73 \times 10^{-6}$	50.7

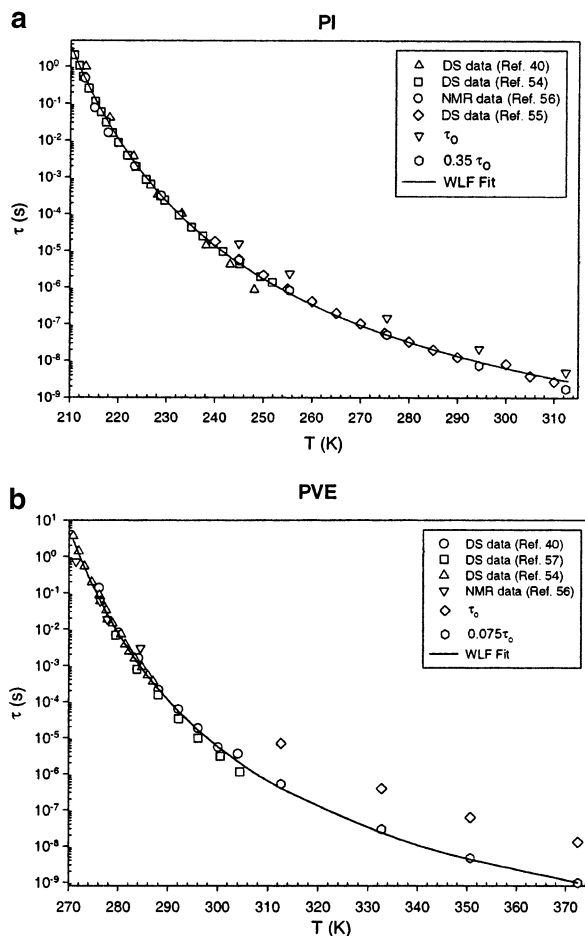


**Figure 3.** Determination of  $\tau_g$  from the temperature dependence of segmental relaxation time for the pure components. (a) For PI,  $\tau_g$  from dielectric spectroscopy (DS) (data of Karatasos et al.,<sup>40</sup> Fytas et al.,<sup>54</sup> and Colmenero et al.<sup>55</sup>) and solid-state NMR (data of Chung et al.<sup>56</sup>) were plotted along with  $\tau_0$ . The WLF equation was fit to  $0.35\tau_0$  and  $\tau_g$  data (solid curve), and  $\tau_g$  was then determined using these WLF coefficients and the ratio  $\tau_g/\tau_0 = 0.35$ . (b) For PVE,  $\tau_g$  from DS (data of Karatasos et al.,<sup>40</sup> Roland et al.,<sup>57</sup> and Fytas et al.<sup>54</sup>) and NMR (data of Chung et al.<sup>56</sup>) were plotted along with  $\tau_0$ . The WLF equation was fit to  $0.075\tau_0$  and  $\tau_g$  data (solid curve), and  $\tau_g$  was then determined using these WLF coefficients and the ratio  $\tau_g/\tau_0 = 0.075$ .

frequency axis) were predicted near quantitatively. The procedure used for calculating  $G_N^0(\phi)$  captures the experimental trend reasonably, as the areas under the predicted and experimental  $G''(\omega)$  are close. It is encouraging to see that the terminal relaxation times of the components, the local maxima in  $G''(\omega)$ , and the widths of these peaks can be predicted in a near quantitative manner by double reptation. All inputs used in LVE predictions for this system are tabulated in Table 3.

**3.4. Thermorheological Behavior.** Since the terminal dynamics of PI/PVE blends are undoubtedly thermorheologically complex,<sup>3–7</sup> it is important to verify

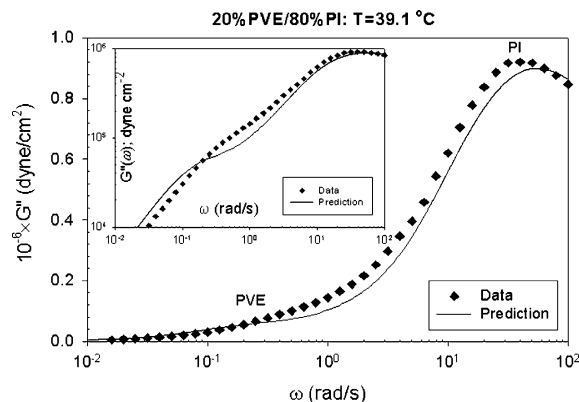


**Figure 4.** PVE/hPI–dPI blend ( $\phi_{\text{PVE}} = 0.2$ ) at 39.1 °C. Calculation of the blend  $G''(\omega)$  using described algorithm is compared to the experimental data of Zawada et al.<sup>5</sup> The inset figure shows the same data and the same predictions, plotted with both axes on logarithmic scales.

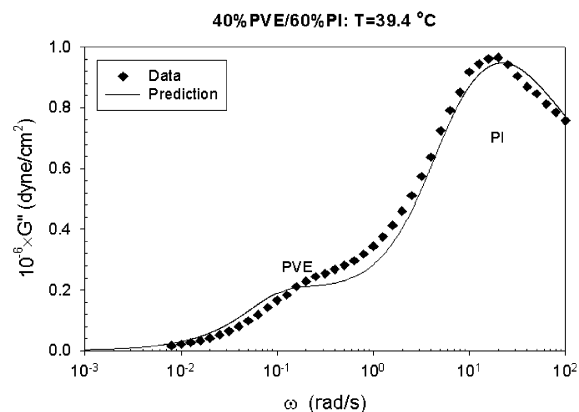


**Figure 5.** PVE/hPI–dPI blend ( $\phi_{\text{PVE}} = 0.4$ ) at 39.4 °C. Calculation of the blend  $G''(\omega)$  using described algorithm is compared to the experimental data of Zawada et al.<sup>5</sup>

that the predictions of double reptation also preserve the complexity seen experimentally. We attempted tTS on experimental data and predictions (Figure 8) for the  $\phi_{\text{PVE}} = 0.80$  blend at two temperatures (29.2 and 39.4 °C), keeping 29.2 °C as the reference temperature. The reptation times of PI and PVE in this blend were 1.63 and 327 s, respectively, at 29.2 °C, and the plateau modulus was  $5.57 \times 10^6$  dyn cm<sup>-2</sup>. For the experimental data (horizontal shift factor  $a_T = 0.215$ ) and the prediction ( $a_T = 0.155$ ), tTS was performed so as to superpose the low-frequency peak arising from the terminal relaxation of PVE chains. In clear agreement with data, the predictions reveal that superposition of the low-frequency relaxation precludes the superposition of the higher frequency relaxation (due to PI chains). We surmise that the origins of the disagreement between the experimental and calculated  $a_T$ 's may lie in our assumption that the components retain their pure WLF coefficients in the blend.

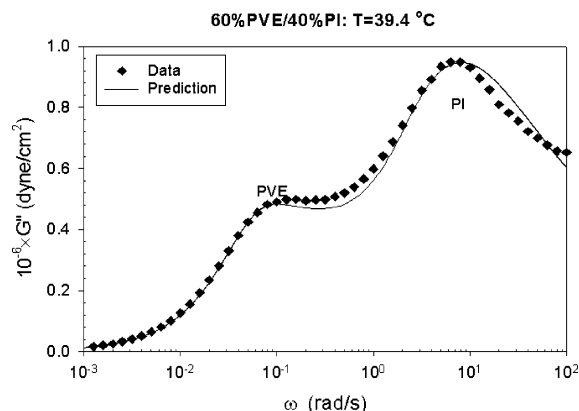


**Figure 6.** PVE/hPI–dPI blend ( $\phi_{\text{PVE}} = 0.6$ ) at 39.4 °C. Calculation of the blend  $G'(\omega)$  using described algorithm is compared to the experimental data of Zawada et al.<sup>5</sup>

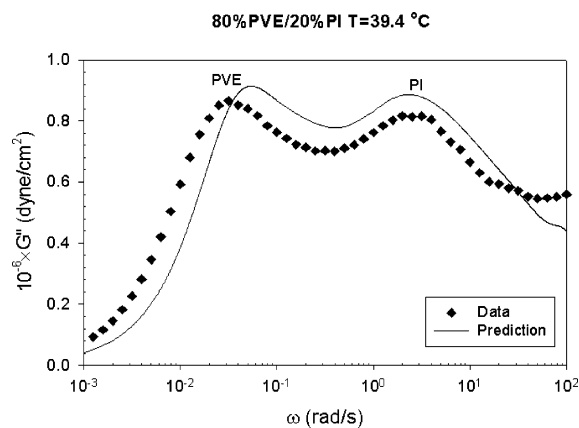


**Figure 7.** PVE/hPI–dPI blend ( $\phi_{\text{PVE}} = 0.8$ ) at 39.4 °C. Calculations of the blend  $G'(\omega)$  using described algorithm is compared to the experimental data of Zawada et al.<sup>5</sup>

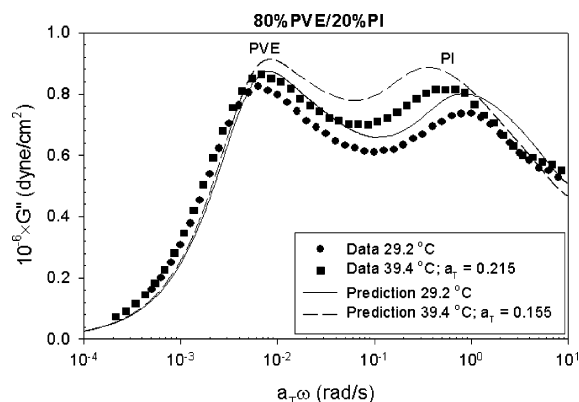


**Figure 8.** Attempt at tTS on blend  $G'(\omega)$  experimental data of Zawada et al.<sup>5</sup> and  $G'(\omega)$  predictions in a blend ( $\phi_{\text{PVE}} = 0.80$ ) at 29.2 °C (the reference temperature) and 39.4 °C. Superposing the low-frequency data (the terminal relaxation of PVE) causes failure of tTS at high frequencies (the terminal relaxation of PI) that is similar in data and prediction.

#### 4. Conclusions

We have applied ideas arising from well-known chain connectivity effects in polymers to determine the effective monomer relaxation times (and hence the effective glass transitions) of the components of a miscible polymer blend. The reptation times of the blend components were calculated from these effective monomer times and then fed into the double reptation model for chain dynamics to calculate  $G'(\omega)$ . We have found very satisfactory agreement between experimental data and

predictions of double reptation without using any adjustable parameters. The well-known result of thermorheological complexity in miscible blends is also predicted. Forthcoming papers will demonstrate the utility of the double reptation model for head-to-head polypropylene/poly(ethylene–propylene) and head-to-head polypropylene/polyisobutylene blends for which we have segmental relaxation data and terminal (oscillatory shear) data.<sup>9,50</sup>

**Acknowledgment.** We gratefully acknowledge financial support from the National Science Foundation (Grant DMR-9977928). J.A.P. thanks Prof. Maria Nobile and Prof. Franco Cocchini (University of Salerno, Salerno, Italy) for kindly introducing him to their FEA algorithm and also thanks Dr. Boris Veytsman (PSU) for discussions. Finally, we also thank both reviewers for having made many constructive suggestions.

#### References and Notes

- (1) Colby, R. H. *Polymer* **1989**, *30*, 1275–1278.
- (2) Roovers, J.; Toporowski, P. M. *Macromolecules* **1992**, *25*, 1096–1102.
- (3) Roovers, J.; Toporowski, P. M. *Macromolecules* **1992**, *25*, 3454–3461.
- (4) Arendt, B. H.; Kannan, R. M.; Zewail, M.; Kornfield, J. A.; Smith, S. D. *Rheol. Acta* **1994**, *33*, 322–336.
- (5) Zawada, J. A.; Fuller, G. G.; Colby, R. H.; Fetters, L. J.; Roovers, J. *Macromolecules* **1994**, *27*, 6861–6870.
- (6) Arendt, B. H.; Krishnamoorti, R.; Kornfield, J. A.; Smith, S. D. *Macromolecules* **1997**, *30*, 1127–1137.
- (7) Arendt, B. H.; Krishnamoorti, R.; Kannan, R. M.; Seitz, K.; Kornfield, J. A.; Roovers, J. *Macromolecules* **1997**, *30*, 1138–1145.
- (8) Pathak, J. A.; Colby, R. H.; Floudas, G.; Jerome, R. *Macromolecules* **1999**, *32*, 2553–2561.
- (9) Pathak, J. A.; Colby, R. H.; Kumar, S. K.; Krishnamoorti, R. In *Binding, D. M., Hudson, N. E., Mewis, J., Piau, J.-M., Petrie, C. J. S., Townsend, P., Wagner, M. H., Walters, K., Eds.; Proceedings of the Thirteenth International Congress on Rheology*; 2000; Vol. 1, pp 257–259.
- (10) Chin, Y. H.; Zhang, C.; Wang, P.; Inglefield, P. T.; Jones, A. A.; Kambour, R. P.; Bendler, J. T.; White, D. M. *Macromolecules* **1992**, *25*, 3031–3038.
- (11) Zetsche, A.; Fischer, E. W. *Acta Polym.* **1994**, *45*, 168–175.
- (12) Kumar, S. K.; Colby, R. H.; Anastasiadis, S. H.; Fytas, G. *J. Chem. Phys.* **1996**, *105*, 3777–3788.
- (13) Lodge, T. P.; McLeish, T. C. B. *Macromolecules* **2000**, *33*, 5278–5284.
- (14) Utracki, L. A. *Polymer Alloys and Blends: Thermodynamics and Rheology*; Carl Hanser Verlag: Munich, 1990.
- (15) Haley, J. C.; Lodge, T. P. *J. Rheol.* **2004**, *48*, 463–486.
- (16) DeGennes, P. G. *J. Chem. Phys.* **1971**, *55*, 572–579.
- (17) Doi, M.; Edwards, S. F. *The Theory of Polymer Dynamics*; Clarendon Press: Oxford, 1986.
- (18) Graessley, W. W. *J. Polym. Sci., Polym. Phys. Ed.* **1980**, *18*, 27–34.
- (19) Rubinstein, M.; Colby, R. H. *J. Chem. Phys.* **1988**, *89*, 5291–5306.
- (20) Marrucci, G. *J. Polym. Sci., Polym. Phys. Ed.* **1985**, *23*, 159–177.
- (21) Viovy, J. L. *J. Phys. (Les Ulis, Fr.)* **1985**, *46*, 847–853.
- (22) Viovy, J. L. *J. Polym. Sci., Polym. Phys. Ed.* **1985**, *23*, 2423–2442.
- (23) Tsenoglou, C. *Polym. Prepr. (Am. Chem. Soc., Div. Polym. Chem.)* **1987**, *28* (2), 185–186.
- (24) Tsenoglou, C. *Macromolecules* **1991**, *24*, 1762–1767.
- (25) desCloizeaux, J. *Europhys. Lett.* **1988**, *5*, 437–442.
- (26) desCloizeaux, J. *Macromolecules* **1990**, *23*, 3992–4006.
- (27) desCloizeaux, J. *Macromolecules* **1990**, *23*, 4678–4687.
- (28) McGrory, W. J.; Tuminello, W. H. *J. Rheol.* **1990**, *34*, 867–890.
- (29) Wasserman, S. H.; Graessley, W. W. *J. Rheol.* **1992**, *36*, 543–572.
- (30) Wasserman, S. H. *J. Rheol.* **1995**, *39*, 601–625.
- (31) Leonardi, F.; Majeste, J.-C.; Allal, A.; Marin, G. *J. Rheol.* **2000**, *44*, 675–692.

- (32) Likhtman, A. E.; McLeish, T. C. B. *Macromolecules* **2002**, *35*, 6332–6343.
- (33) Fetters, L. J.; Lohse, D. J.; Colby, R. H. In *Physical Properties of Polymers Handbook*; Mark, J. E., Ed.; AIP Press: Woodbury, NY, 1996; Chapter 24, pp 335–340.
- (34) Composto, R. J.; Kramer, E. J.; White, D. M. *Polymer* **1990**, *31*, 2320–2328.
- (35) Composto, R. J.; Kramer, E. J.; White, D. M. *Macromolecules* **1992**, *25*, 4167–4174.
- (36) Zawada, J. A.; Ylitalo, C. M.; Fuller, G. G.; Colby, R. H.; Long, T. E. *Macromolecules* **1992**, *25*, 2896–2902.
- (37) Kim, E.; Kramer, E. J.; Osby, J. O. *Macromolecules* **1995**, *28*, 1979–1989.
- (38) Stockmayer, W. H. In *Molecular Fluids (Proceedings of NATO Summer School, Les Houches)*; Balian, R., Weill, G., Eds.; Gordon and Breach: London, 1976.
- (39) Rubinstein, M.; Colby, R. H. *Polymer Physics*; Oxford University Press: New York, 2003.
- (40) Kamath, S.; Colby, R. H.; Kumar, S. K.; Karatasos, K.; Floudas, G.; Fytas, G.; Roovers, J. *J. Chem. Phys.* **1999**, *111*, 6121–6128.
- (41) Salaniwal, S.; Kant, R.; Colby, R. H.; Kumar, S. K. *Macromolecules* **2002**, *35*, 9211–9218.
- (42) Kant, R.; Kumar, S. K.; Colby, R. H. *Macromolecules* **2003**, *36*, 10087–10094.
- (43) Haley, J. C.; Lodge, T. P.; He, Y.; Ediger, M. D.; von Meerwall, E. D.; Mijovic, J. *Macromolecules* **2003**, *36*, 6142–6151.
- (44) He, Y.; Lutz, T. R.; Ediger, M. D. *J. Chem. Phys.* **2003**, *119*, 9956–9965.
- (45) Zawada, J. A. Component Contributions to the Dynamics of Miscible Polymer Blends. Ph.D. Thesis, Stanford University, Stanford, CA, 1993.
- (46) Zawada, J. A.; Fuller, G. G.; Colby, R. H.; Fetters, L. J.; Roovers, J. *Macromolecules* **1994**, *27*, 6851–6860.
- (47) Fox, T. G. *Bull. Am. Phys. Soc.* **1956**, *2*, 123–123.
- (48) Ferry, J. D. *Viscoelastic Properties of Polymers*, 3rd ed.; Wiley: New York, 1980.
- (49) Nobile, M. R.; Cocchini, F. *Rheol. Acta* **2001**, *40*, 111–119.
- (50) Pathak, J. A. Miscible Polymer Blend Dynamics. Ph.D. Thesis, The Pennsylvania State University, 2001.
- (51) Balsara, N. P. In *Physical Properties of Polymers Handbook*; Mark, J. E., Ed.; AIP Press: Woodbury, NY, 1996; Chapter 19, pp 257–268.
- (52) Doi, M. *J. Polym. Sci., Polym. Lett. Ed.* **1981**, *19*, 265–273.
- (53) Pathak, J. A.; Colby, R. H.; Kamath, S. Y.; Kumar, S. K.; Stadler, R. *Macromolecules* **1998**, *31*, 8988–8997.
- (54) Fytas, G.; Anastasiadis, S. H.; Karatasos, K.; Hadjichristidis, N. *Phys. Scr.* **1993**, *T49*, 237–241.
- (55) Alvarez, F.; Alegria, A.; Colmenero, J. *Macromolecules* **1997**, *30*, 597–604.
- (56) Chung, G. C.; Kornfield, J. A.; Smith, S. D. *Macromolecules* **1994**, *27*, 964–973.
- (57) Ngai, K. L.; Roland, C. M. *Macromolecules* **1995**, *28*, 4033–4035.

MA049628A